Journal of Power Sources 218 (2012) 34–38

Contents lists available at SciVerse ScienceDirect

Journal of Power Sources

journal homepage: www.elsevier.com/locate/jpowsour

In situ Raman spectroscopy of layered solid solution Li_2MnO_3–$LiMO_2$ (M = Ni, Mn, Co)

Gurpreet Singh [a,*], W.C. West [b], J. Soler [b], Ram S. Katiyar [a]

[a] Department of Physics, Institute for Functional Nanomaterials, University of Puerto Rico, San Juan, PR 00936-8377, USA
[b] Jet Propulsion Laboratory, California Institute of Technology, Pasadena, CA 91109, USA

HIGHLIGHTS

- In situ Raman spectroscopy of layered solid solution of Li_2MnO_3–$LiMO_2$ (M = Ni, Mn, and Co).
- Impedance decrease steadily and reaches minimum at 4.47 V
- Less steep increase in impedance as cell voltage traversed the first charge 4.5 V plateau.
- Lithium extraction occur from transition metals as well as lithium layers in 4.1–4.4 V voltage range.
- Extraction of oxygen along with lithium ions from the transition metal layers takes place after 4.5 V.

ARTICLE INFO

Article history:
Received 26 April 2012
Received in revised form
22 June 2012
Accepted 22 June 2012
Available online 2 July 2012

Keywords:
Cathode
Solid solution
Lithium ion battery
Raman spectroscopy

ABSTRACT

Lithium rich manganese oxide based materials are emerging as possible high energy density cathode materials for lithium ion batteries. In the present research, we have investigated the first charge/discharge profile behavior of $Li_{1.2}Ni_{0.175}Co_{0.1}Mn_{0.52}O_2$ via in situ Raman spectroscopy. X-ray diffraction studies confirm the presence of cation ordering in the transition metal layers. Scanning electron microscopy shows the homogeneous distribution of highly dense spherical agglomerates of ~5 μm size. Steady decrease in impedance up to ~4.5 V followed by a less steep increase as the cell voltage traversed the first charge cycle has been confirmed by electrochemical impedance spectroscopy. Raman spectroscopy shows that the extraction of lithium takes place from both the transition metal layers as well as lithium layers in the voltage range of 4.1–4.4 V. The oxygen removal becomes severe in the voltage range of 4.55–4.6 V, after which the diffusion of the transition metal ions to the vacant sites takes place.

1. Introduction

Lithium rich manganese based cathodes have been the focus of research in the past few years due to their potential application for next generation electrode materials [1,2]. The crystallographic structure of these materials has been studied vigorously and it has been shown that these materials can be presented in a more simplified manner as a composite of the two different components viz. Li_2MnO_3 and $LiMO_2$ (where M = Co, Ni, Mn or combination of each other) [3]. Various stoichiometries with different combinations of Li_2MnO_3 and $LiMO_2$ [e.g. $xLi_2MnO_3 \cdot (1-x)LiMO_2$] have been studied in the recent past [4,5]. Among the various compounds $Li_{1.2}Ni_{0.2}Mn_{0.6}O_2$ [$0.5Li_2MnO_3 \cdot 0.5LiNi_{0.5}Mn_{0.5}O_2$] and $Li_{1.2}Mn_{0.54}Ni_{0.13}Co_{0.13}O_2$ [$0.5Li_2MnO_3 \cdot 0.5LiNi_{0.33}Mn_{0.33}Co_{0.33}O_2$] have been studied by many authors [6,7]. The use of the cobalt helps in reducing the electrode polarization [7]. The mechanism behind the electrochemical activity of Li_2MnO_3 has also been studied [8]. Li_2MnO_3 is known to be electrochemically inactive because of the presence of Mn in its +4 oxidation state. However charging this material above 4.5 V can apparently electrochemically activate the material due to the extraction of Li and O, which in turn leads to the formation of the MnO_2 host structure in the compound which can then reversibly intercalate lithium ions [9].

One of the drawbacks with such materials is their high irreversible capacity, which has been focus of research in many scientific groups [10,11]. Various mechanisms have been given for the explanation of the first cycle charge profile behavior in these electrode system using different characterization tools. Recent detailed studies on the first cycle charging mechanism have suggested the simultaneous oxygen and lithium removal during the first cycle voltage plateau, followed by the cation migration from transition metal layers to the lithium layers and some of the reversible capacity in such materials is due to the

* Corresponding author. Tel.: +1 787 751 4210; fax: +1 787 764 2571.
E-mail address: singhgurpreet268@yahoo.com (G. Singh).

0378-7753/$ – see front matter © 2012 Elsevier B.V. All rights reserved.
http://dx.doi.org/10.1016/j.jpowsour.2012.06.083

redox reaction of the oxygen during charge [12]. Armstrong et al. have suggested that the first cycle flat charge profile is associated with the oxygen loss from the surface which is further accompanied by the diffusion of the transition metal ions from the surface to the bulk [13]. Tran et al. in their study on the first cycle behavior have ruled out the model of the migration of the oxygen from the bulk to the surface, however they also considered that the plateau is associated with the migration of the transition metal ions from the surface to the bulk [14]. Bommel et al. in their recent studies have focused the research on the stage at which the removal of the lithium ions from the transition metal layers takes place [15]. It has been shown that the lithium extraction from the transition metal layer takes place at the start of oxygen release and not at the start of charge. This study is in contrast to the study carried by Grey et al. suggesting lithium removal from the transition metal layer at the start of charging [16]. Experiments have been carried out to quantify the amount of utilizable lithium that is made available for the corresponding anodes when employing Li_2MnO_3–$LiMO_2$ as cathodes. It has been shown that almost none of the cathode irreversible charge capacity resulted in lithiation of the anode, demonstrating that lithium released from the cathode (and made available at the anode) during the first charge is not proportionate to the cathode charge capacity [11]. Another detailed study on $Li_{1.2}Ni_{0.13}Co_{0.13}Mn_{0.54}O_2$ has been reported by Yabuuchi et al. and it has been shown that some of the capacity in such kind of electrode materials is due to the electrochemical redox reaction of the oxygen molecules at the surface of the electrode [17].

Understanding the above-mentioned aspects, which are associated with the first cycle charge behaviors, is necessary to understand and reduce the first cycle irreversible capacity loss in such materials. Raman spectroscopy has been considered as an effective tool in order to understand the local structural changes occurring in the material [18]. In the present study we have used the in situ Raman spectroscopy to investigate the mechanisms associated with first cycle charge profile. $Li_{1.2}Ni_{0.175}Co_{0.1}Mn_{0.52}O_2$ has been examined as a material of choice in the present in situ Raman spectroscopy study.

2. Experimental

The in situ Raman coin cells were prepared as follows. Al clad stainless steel CR2032 coin cell cases were punched with 0.09,375 in. or 0.1875 in. diameter holes with a metal hole puncher. The holes were covered on the inside of the cases with either a thin quartz or MgO window, held in place with a fluoroelastomer caulk. The inside of the cases including the windows were spray coated with a cathode slurry consisting of 80 wt% cathode powder ($Li_{1.2}Ni_{0.175}Co_{0.1}Mn_{0.52}O_2$, Toda), 10 wt % C black (Shawinigan), and 10 wt % poly(vinylene difluoride) (PVDF) binder (Sigma Aldrich, MW_{avg}=534,000) in N-methyl-2-pyrrolidinone (NMP) (Sigma Aldrich) with an active mass loading of approximately 4.6–15.0 mg cm^{-2} after drying. Care was taken during spray coating to assure that the top as well as the edges of the window were spray coated to assure that electronic continuity was maintained between the top of the cathode film on the window to the coin cell case edge. Following coating and air drying, the cases were vacuum dried overnight at 100 °C. Prior to assembly, the continuity between the cell case and the cathode on the window was verified by probing electronic resistance between the coin cell case to the cathode film on the quartz or MgO window with a ohmmeter.

After the preparation of the cathodes, the cells were assembled in an argon glovebox by placing a 20 μm thick Tonen separator held in place with a polyethylene o-ring onto the cell case over the cathode film. A 100 μl of electrolyte consisting of 1 M $LiPF_6$ in ethylene carbonate:dimethyl carbonate:diethyl carbonate (EC:DMC:DEC) (1:1:1 vol %) was pipetted into the cell. A lithium counter electrode, stainless steel shim, and wave spring were placed on the separator, and the entire assembly was then capped and crimped.

The X-ray diffraction (XRD) measurements were carried out on the cathode powder using a Siemens D500 diffractometer run in the theta-2 theta geometry, with a Cu anode (λ = 1.541 Å) at an accelerating voltage of 40 kV and a tube current of 20 mA. Surface morphology was studied using an FEI Nova NanoSEM 600 field-emission electron microscope.

Electrochemical Impedance Spectroscopy (EIS) measurements of coin cells were performed at room temperature as a function of state of charge using a potentiostat/galvanostat/frequency response analyzer (Biologic VMP2). The applied AC signal was 2 mV over a frequency range of 200 kHz–50 mHz under potentiostatic conditions.

Galvanostatic charge/discharge measurements have been carried out on the samples in the voltage range of 4.8–2.0 V at a charge/discharge rate of C/10. Raman spectroscopy was carried out utilizing a T64000 Raman spectrometer from Horiba Inc. and an Ar ion laser with 514.5 nm as excitation source in the wavenumber range of 200–800 cm^{-1}. Raman spectra of the $Li_{1.2}Ni_{0.175}Co_{0.1}Mn_{0.52}O_2$ cathode material was collected while charging and discharging after a voltage step of 0.1 V in the voltage range of OCV – 4.8 V and 4.8–3.0 V.

3. Results and discussion

The cathode powder microstructure was characterized by uniform, spherical particles approximately 5 μm in diameter coalesced from submicron primary particles (Fig. 1). The X-ray diffraction pattern of the $Li_{1.2}Ni_{0.175}Co_{0.1}Mn_{0.52}O_2$ powder was well indexed to the layered solid solution Li_2MnO_3–$LiMO_2$ (M = Ni, Mn, Co), with no additional diffraction peaks discerned (Fig. 2). Weak peaks at 2θ of 21° to 25° that were not indexed to the $R\bar{3}m$ symmetry were consistent with cation ordering that occurs in the transition metal layer [1].

The impedance of the cathode on the first charge cycle was measured as a function of state of charge. The Bode plots of the modulus of impedance $|Z|$ versus log frequency are shown in Fig. 3. As the cell voltage was increased on the first charge cycle, a clear decrease in impedance over virtually the entire frequency range was observed from the initial as-prepared uncharged state up to approximately 4.47 V. At cell voltages from about 4.47 V to 4.63 V, the impedance was a much weaker function of state of charge, with marked increases in the low frequency impedances at the highest state of charge. The modulus of impedance taken at 100 Hz was plotted versus open circuit voltage (Fig. 4), again demonstrating the trend that as the cathode was charged, the impedance steadily decreased to a minimum at ca. 4.47 V followed by a less steep increase as the cell voltage traversed the first charge cycle 4.5 V plateau.

Raman spectra during galvanostatic charging and discharging of the material between OCV – 4.8 V and 4.8–3.0 V are shown in Fig. 5(a) and (b), respectively. The corresponding charge/discharge profiles are shown in Fig. 6(a) and (b), respectively.

Three major peaks in the Raman spectrum have been observed at 445, 487 and 604 cm^{-1} for the sample at open circuit voltage. The highest intensity peak at 604 cm^{-1} is observed to be quite broad along with shoulder in between 650 and 700 cm^{-1}. The spectrum is quite similar to that reported in the earlier reports on similar kind of solid solution [19]. In the present study peaks present at 604 and 487 cm^{-1} are assigned to the A_{1g} and E_g modes, respectively. However the peak present at ~445 cm^{-1} shows the explicit presence of Li_2MnO_3 short range superlattice ordering (space group C2/m).

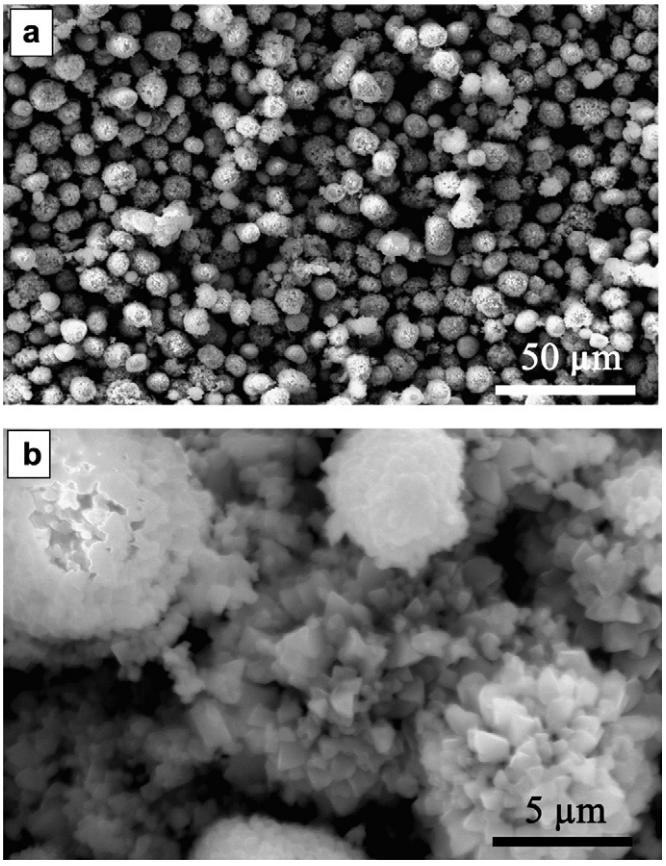

Fig. 1. Scanning electron micrographs of the $Li_{1.2}Ni_{0.175}Co_{0.1}Mn_{0.52}O_2$ cathode powder at a) 500× magnification and b) 5000× magnification.

With the increase in voltage (Fig. 5(a)) a new peak starts evolving in between the 500 and 600 cm^{-1} at 4.1 V, and a well pronounced peak at 544 cm^{-1} has been observed at 4.3 V. On further increasing the voltage to 4.8 V the intensity of this peak

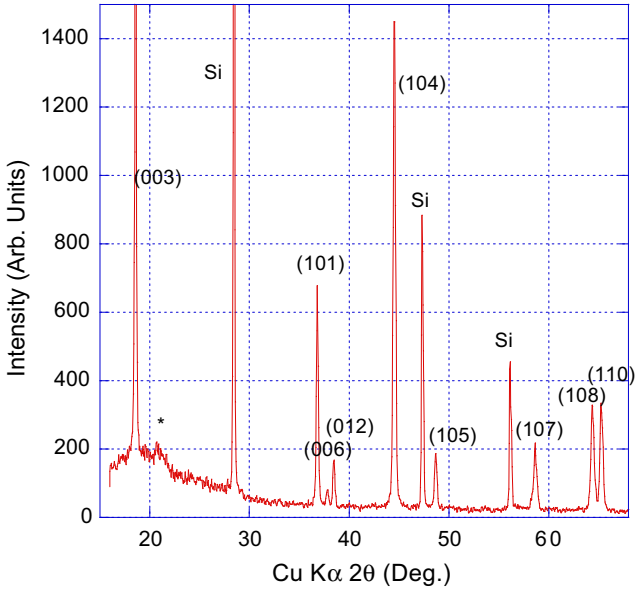

Fig. 2. X-ray diffraction data of the $Li_{1.2}Ni_{0.175}Co_{0.1}Mn_{0.52}O_2$ cathode powders. The asterisk indicates reflections associated with cation superlattice ordering. Where (*) represents the cation ordering that occurs in the transition metal layers of the crystal structure.

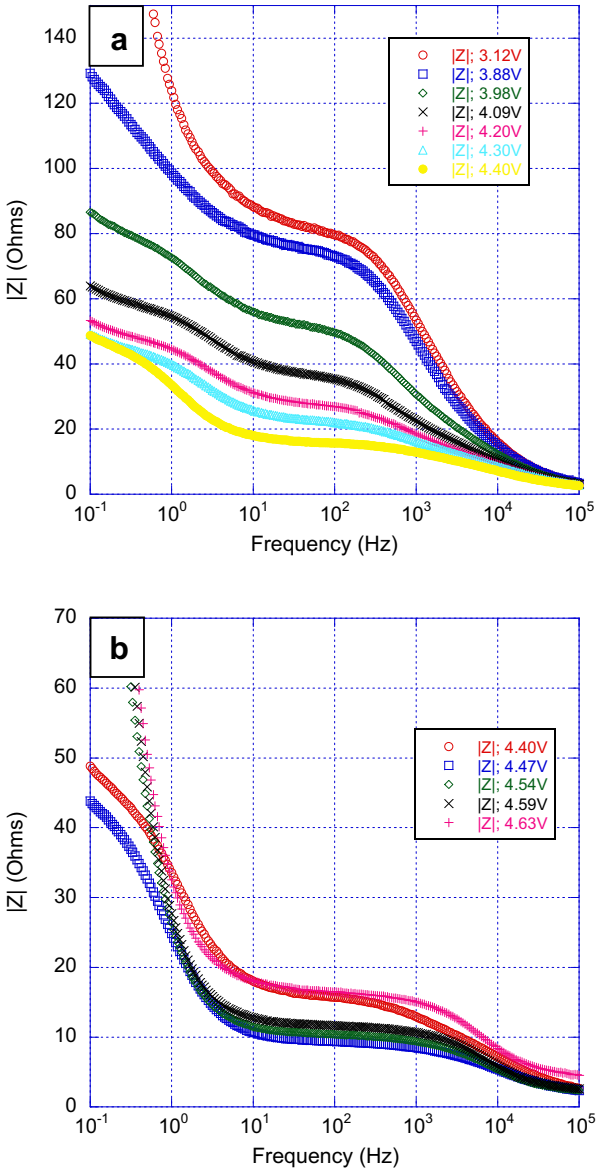

Fig. 3. Bode plots of modulus of impedance $|Z|$ versus log frequency for cell voltages from a) 3.12–4.40 V, and b) 4.40–4.63 V.

decreases significantly, showing the rearrangement of the ions in the structure in the higher voltage region. Another major change in the spectrum has been observed for the peak present at 604 cm^{-1}. It has been observed that with the increase in voltage the peak intensity decreases and the spectrum is left with a minor signature of the peak after 4.5 V. The peak at 604 cm^{-1} disintegrates with the increase in voltage, showing the change in local environment with the extraction of lithium or increase in voltage. A change in the peak present at 445 cm^{-1}, which corresponds to the explicit presence of the Li_2MnO_3 in the structure, has been observed after 4.1 V. It is not distinguishable from the peak present at 487 cm^{-1}. However this peak again becomes distinguishable at 4.7 V, showing the rearrangement of the ions in the higher voltage region, i.e. 4.6–4.8 V. Such a clear distinction of the peaks can be observed easily during the discharging of the sample (Fig. 5(b)). Suppression in the background intensity of the signal has also been observed at the beginning of the discharge. During discharge, the peaks present at higher wavenumbers reappear and become pronounced at the end of discharge.

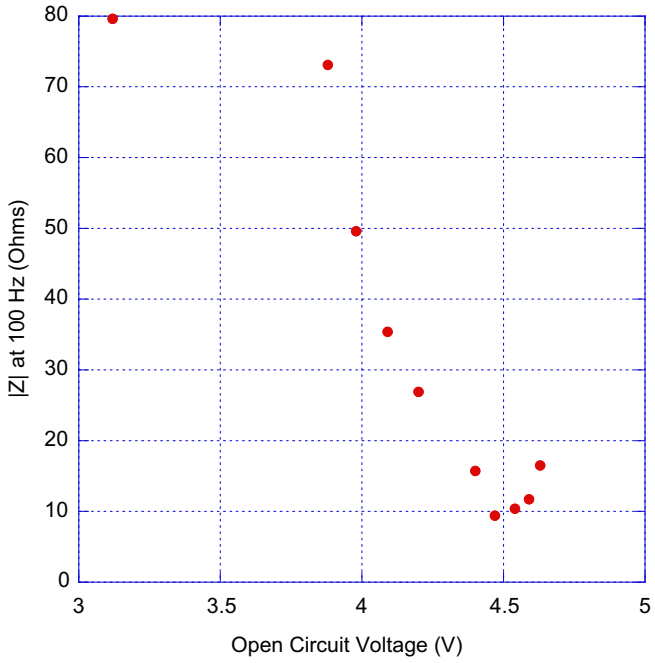

Fig. 4. Modulus of impedance |Z| versus open circuit voltage on the first charge cycle.

Raman spectra of Li_2MnO_3 belonging to the C2/m space group symmetry has already been reported in the literature and show bands at 248, 308, 332, 369, 413, 438, 493, 568 and 612 cm^{-1} [18]. In one of the earlier studies on these composite cathode materials it has been shown that the peaks become broad and shift towards the lower wavenumbers with the increase in Co content in the materials [19]. In the present study, a shoulder to the higher intensity peak has been attributed to the local distortion, which is caused by the decrease in structural symmetry [20]. With the increase in voltage, an emergence of the new peak at ~544 cm^{-1}, shows the oxidation of the Ni^{2+} ions present in the structure [21]. Raman spectra of $LiNiO_2$, in which Ni is present in +3 oxidation state shows two Raman active modes at 545 and 465 cm^{-1}. This is also consistent with the electrochemical results in which monotonic increase in the voltage corresponds to the oxidation of the Ni^{2+} ions present in the sample (Fig. 6(a)). Such an oxidation is reported to occur in the voltage range OCV – 4.4 V. Oxidation of Ni^{2+} ions is clearly reflected as a broad peak in the differential capacity versus voltage curves as shown in Fig. 7. In recent studies, it has been shown that the Ni^{2+} ion oxidation leads to the lithium ions removal from the lithium layers in the voltage region of OCV – 4.4 V [15]. However, in the present study a change in the peak present at 445 cm^{-1}after 4.1 V shows a high possibility of extraction of lithium from the transition metal layers around 4.1 V. Earlier studies show that the formation of tri-vacancy leads to the movement of the lithium ions from the transition metal layers to the vacant site at lower potentials 2.92 V [16]. Contrary in the present research work, no change in the spectrum between 400 and 525 cm^{-1} up to 4.1 V is observed which rules out such movement of the Li ions from transition metal sites to the tetrahedral sites at low potentials. Above 4.1 V, the peak present at 445 cm^{-1} is no more distinguishable from the peak present at 487 cm^{-1}. A change in the slope of the charge profile has also been observed after 4.1 V. This might be attributed to the start of the lithium extraction from the transition metal layers near 4.1–4.3 V region. These changes in the spectrum, i.e. evolution of the peak at 544 cm^{-1} and the change in peak at 445 cm^{-1}, are more pronounced at 4.3 V. A sudden increase in background of the Raman signal in the lower wavenumber range

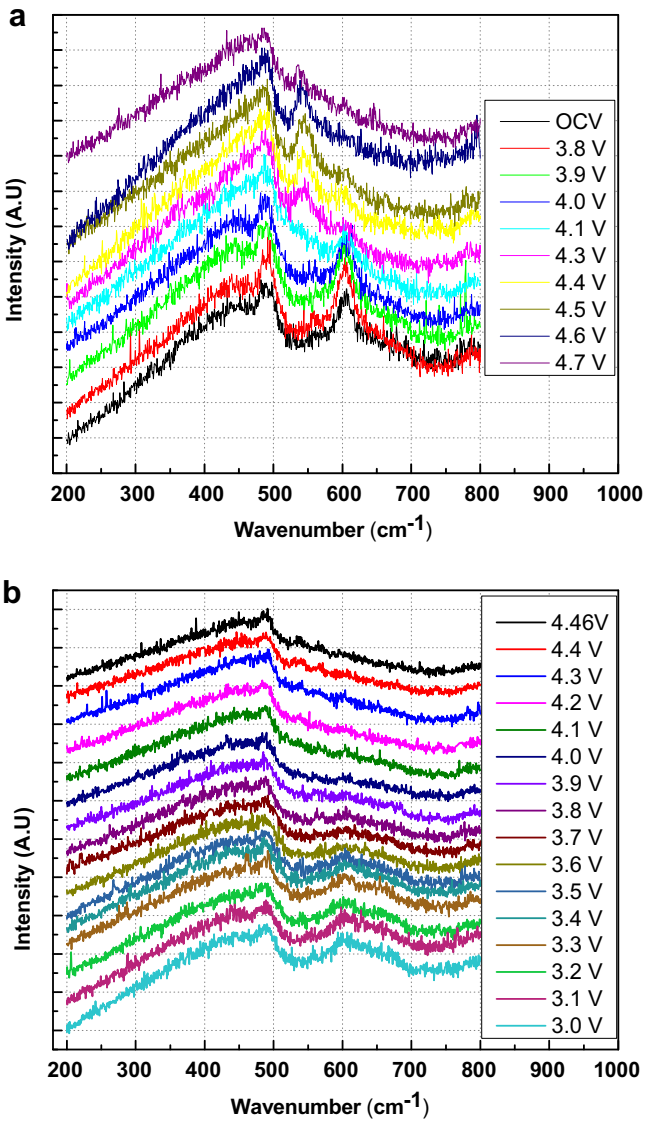

Fig. 5. In situ Raman spectra of the $Li_{1.2}Ni_{0.175}Co_{0.1}Mn_{0.52}O_2$ cathode powder (a) during first cycle charging and (b) during first cycle discharging collected after a voltage interval of 0.1 V.

(200–500 cm^{-1}) with the increase in voltage at 4.5 V has been observed, which is attributed to the increase in the oxygen vacancies in the structure that should account for the photoluminescence in the sample. No change in the peak present at 544 cm^{-1} has been observed in the voltage range of 4.5–4.6 V. These observations show the extraction of the oxygen ions from the structure along with the removal of the lithium ions from the transition metal layers after 4.5 V. In the 4.6–4.8 V range, a decrease in the background signal towards the higher wavenumber has been observed and is attributed to the filling of the vacant sites in the structure. According to the transition metal ion diffusion mechanism, the diffusion of the transition metal ions from the surface to the bulk should take place. A sudden decrease in the intensity of the peak at 544 cm^{-1} (reflecting Ni^{3+} ions) has been observed after 4.6 V along with the decrease in the background signal, which justifies the diffusion of the transition metal ions from the surface to the bulk. Raman spectra during the discharging of the sample show the emergence of the peak at 604 cm^{-1} that corresponds to insertion of the lithium ions back in the structure, without any other major change.

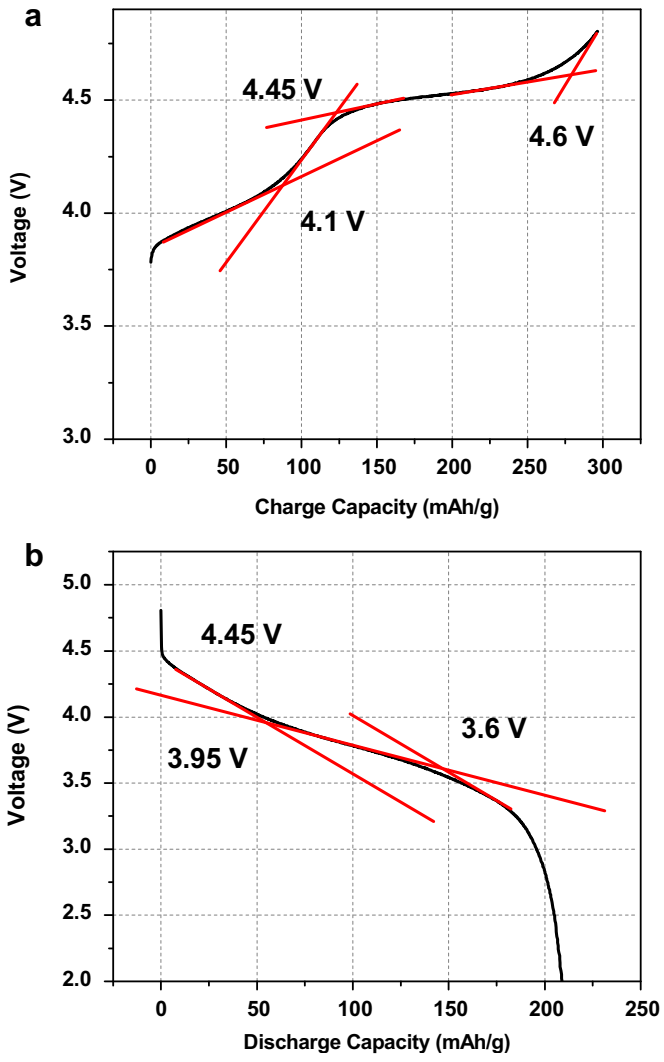

Fig. 6. (a) First cycle charge profile of the $Li_{1.2}Ni_{0.175}Co_{0.1}Mn_{0.52}O_2$ cathode powder (b) first cycle discharge profile of the $Li_{1.2}Ni_{0.175}Co_{0.1}Mn_{0.52}O_2$ cathode powder.

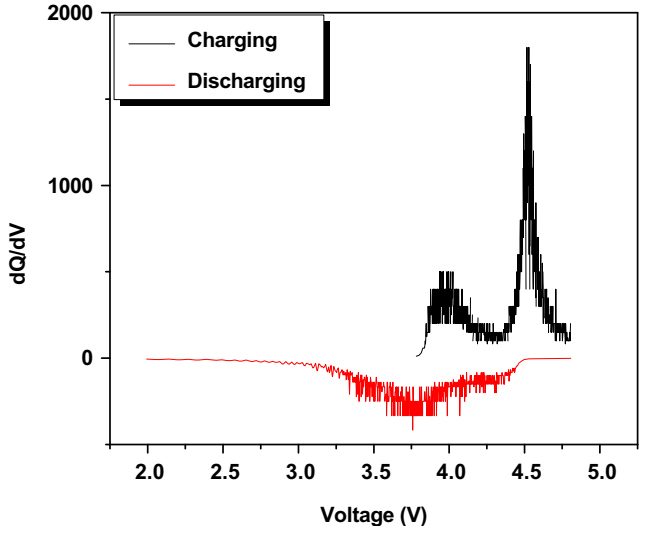

Fig. 7. Variation of differential capacity w.r.t. voltage during first charge/discharge cycle.

4. Conclusions

In summary, it can be concluded that the lithium extraction from the lithium layers starts at the beginning of the charge profile during the oxidation of the transition metal ions, as shown by the emergence of new peak at 544 cm^{-1}. In the voltage range of 4.1–4.4 V extraction of the lithium takes place from both the transition metal layers as well as lithium layers, reflected by the change in peaks at 445 and 544 cm^{-1}. After 4.5 V, the extraction of the lithium from the transition metal layers is accompanied by the oxygen ion removal. The oxygen ion removal becomes severe in the voltage range of 4.55–4.6 V, after which the diffusion of the transition metal ions to the vacant sites takes place. Such an occupation of the vacant sites by the transition metal ions in the structure may lead to the irreversible capacity of the cathode material. These results are well supported by the EIS study that shows the decrease in the impedance up to 4.5 V region with the gradual increase afterwards.

Acknowledgements

The financial support from NASA-URC (NNX08BA48A) grant to University of Puerto Rico is gratefully acknowledged.

This work was partially carried out at the Jet Propulsion Laboratory, California Institute of Technology, under contract with the National Aeronautics and Space Administration. The authors acknowledge the funding support of NASA's Space Power Systems Program.

References

[1] Michael M. Thackeray, Sun-Ho Kang, Christopher S. Johnson, John T. Vaughey, Roy Benedek, S.A. Hackney, J. Mater. Chem. 17 (2007) 3112–3125.
[2] Zhonghua Lu, L.Y. Beaulieu, R.A. Donaberger, C.L. Thomas, J.R. Dahn, J. Electrochem. Soc. 149 (2002) A778–A791.
[3] C.S. Johnson, J.-S. Kim, C. Lefief, N. Li, J.T. Vaughey, M.M. Thackeray, Electrochem. Commun. 6 (2004) 1085–1091.
[4] T.A. Arunkumar, Y. Wu, A. Manthiram, Chem. Mater. 19 (2007) 3067–3073.
[5] Y. Wu, A. Manthiram, Solid State Ionics 180 (2009) 50–56.
[6] C.H. Lei, J. Bareno, J.G. Wen, I. Petrov, S.-H. Kang, D.P. Abraham, J. Power Sources 178 (2008) 422–433.
[7] S.-H. Kang, P. Kempgens, S. Greenbaum, A.J. Kropf, K. Amine, M.M. Thackeray, J. Mater. Chem. 17 (2007) 2069–2077.
[8] Alastair D. Robertson, Peter G. Bruce, Chem. Mater. 15 (2003) 1984–1992.
[9] Zhonghua Lu, J.R. Dahn, J. Electrochem. Soc. 149 (2002) A815–A822.
[10] Z.Q. Deng, A. Manthiram, J. Phys. Chem. C 115 (2011) 7097–7103.
[11] W.C. West, R.J. Staniewicz, C. Ma, J. Robak, J. Soler, M.C. Smart, B.V. Ratnakumar, J. Power Sources 196 (2011) 9696–9701.
[12] Atsushi Ito, Kaoru Shoda, Yuichi Sato, Masaharu Hatano, Hideaki Horie, Yasuhiko Ohsawa, J. Power Sources 196 (2011) 4785–4790.
[13] A. Robert Armstrong, Michael Holzapfel, Petr Novák, Christopher S. Johnson, Sun-Ho Kang, Michael M. Thackeray., Peter G. Bruce, J. Am. Chem. Soc. 128 (2006) 8694–8698.
[14] N. Tran, L. Croguennex, M. Menetrier, F. Weill, Ph. Biensan, C. Jordy, C. Delmas, Chem. Mater. 20 (2008) 4815–4825.
[15] Andrew van Bommel, L.J. Krause, J.R. Dahn, J. Electrochem. Soc. 158 (2011) A731–A735.
[16] C.P. Grey, W. Yoon, J. Reed, G. Ceder, Electrochem. Solid-State Lett. 7 (2004) A290–A 293.
[17] Naoaki Yabuuchi, Kazuhiro Yoshii, Seung-Taek Myung, Izumi Nakai, Shinichi Komaba, J. Am. Chem. Soc. 133 (2011) 4404.
[18] Y.W. Yu Denis, Katsunori Yanagida, J. Electrochem. Soc. 158 (2011) A1015–A1022.
[19] Lianqi Zhang, Kazunori Takada, Narumi Ohta, Katsutoshi Fukuda, Minoru Osada, Lianzhou Wang, Takayoshi Sasaki, Mamoru Watanabe, J. Electrochem. Soc. 152 (2005) A171–A178.
[20] Zhe Li, Fei Du, Xiaofei Bie, Dong Zhang, Yongmao Cai, Xinran Cui, Chunzhong Wang, Gang Chen, Yingjin Wei, J. Phys. Chem. C. 114 (2010) 22751–22757.
[21] P. Kalyani, N. Kalaiselvi, Sci. Tech. Adv. Mater. 6 (2005) 689–703.